Soft Matter

RSC Publishing

PAPER

View Article Online
View Journal

Collective alignment of nanorods in thin Newtonian films†

Cite this: DOI: 10.1039/c3sm51467f

Yu Gu,[a] Ruslan Burtovyy,[a] James Townsend,[a] Jeffery R. Owens,[b] Igor Luzinov[a] and Konstantin G. Kornev*[a]

In this paper, we provide a complete analytical description of the alignment kinetics of magnetic nanorods in magnetic field. Nickel nanorods were formed by template electrochemical deposition in alumina membranes from a dispersion in a water–glycerol mixture. To ensure uniformity of the dispersion, the surface of the nickel nanorods was covered with polyvinylpyrrolidone (PVP). A 40–70 nm coating prevented aggregation of the nanorods. These modifications allowed us to control alignment of the nanorods in a magnetic field and test the proposed theory. An orientational distribution function of nanorods was introduced. We demonstrated that the 0.04% volume fraction of nanorods in the glycerol–water mixture behaves as a system of non-interacting particles. However, the kinetics of alignment of a nanorod assembly does not follow the predictions of the single-nanorod theory. The distribution function theory explains the kinetics of alignment of a nanorod assembly and shows the significance of the initial distribution of nanorods in the film. It can be used to develop an experimental protocol for controlled ordering of magnetic nanorods in thin films.

Received 25th May 2013
Accepted 12th July 2013

DOI: 10.1039/c3sm51467f

www.rsc.org/softmatter

Introduction

In recent years, magnetic nanorods have attracted great attention due to the breadth of applications their unique magnetic and geometrical features open for medicine,[1,2] sensors,[3,4] optofluidics,[5,6] and microrheology.[7–10] In particular, magnetic nanorods offer new opportunities in manufacturing of multifunctional composites with unprecedented magnetic and mechanical properties.[11–13] Composites with ordered nanorods are especially attractive for different high-tech applications.[14,15] At the end of the last century, the problem of particle alignment in liquid media was actively discussed in applications to manufacturing of high-density recording films and discs.[16–18] However, the strategy for nanorod alignment in macroscopic materials has not been developed and this remains the main challenge in materials engineering and processing. This problem requires understanding the kinetics of alignment of an assembly of nanorods. It also requires the development of advanced physicochemical methods of nanorod stabilization against agglomeration. In this paper, we address these problems using nickel nanorods as a model. To ensure uniformity of dispersion, the surface of nickel nanorods was covered with polyvinylpyrrolidone (PVP). A 40–70 nm coating prevents aggregation of nanorods dispersed in a water–glycerol mixture. An orientational distribution function of nanorods is introduced and then studied both theoretically and experimentally. We show that the kinetics of alignment of a nanorod assembly does not follow the predictions of the single-nanorod theory and significantly depends on the initial distribution of nanorods in the film.

[a]Department of Materials Science and Engineering, Clemson University, Clemson, SC, 29678, USA. E-mail: kkornev@clemson.edu; Tel: +1 8646566541

[b]Air Force Research Laboratory, Airbase Technologies Division, Airbase Sciences Branch, TyndallAFB, Panama City, Florida 32403, USA

† Electronic supplementary information (ESI) available. See DOI: 10.1039/c3sm51467f

Theory

In the manufacturing of thin nanocomposite films, nanorods are aligned in the film plane by applying an external magnetic field parallel to the film surface. In this paper, only Newtonian liquids with constant viscosity η are considered. We restrict ourselves to the case of dilute dispersions in which the interactions between nanorods are weak and can be ignored. To control the kinetics of nanorod alignment, one first needs to understand the kinetics of alignment of a single nanorod.

Kinetics of alignment of a single nanorod

The orientation of a single nanorod in an external magnetic field can be described using Cartesian coordinates as shown in Fig. 1, where $\boldsymbol{m}$ is the magnetic moment, which lies along the nanorod axis, and $\boldsymbol{B}$ is the external magnetic field. Vector $\boldsymbol{m}$ makes angle θ with vector $\boldsymbol{B}$, vector $\boldsymbol{B}$ makes angle α with the x-axis, and vector $\boldsymbol{m}$ makes angle φ with the x-axis. Thereafter, nanorod orientation is defined by the orientation of its magnetic moment $\boldsymbol{m}$.

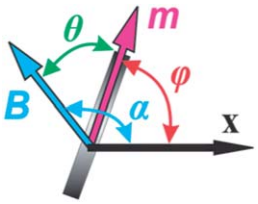

Fig. 1 Basic vectors associated with the magnetic nanorod and magnetic field.

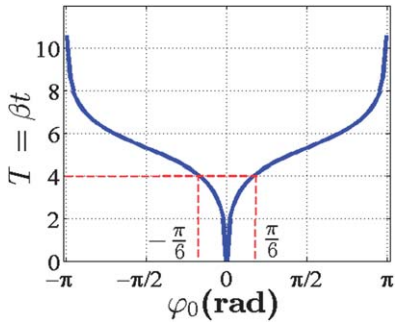

Fig. 2 Dimensionless time needed for a nanorod to reach its equilibrium orientation as a function of the initial orientation of the nanorod φ_0. The dashed lines help to understand the meaning of this master curve explaining the example in the text.

In most cases of composite manufacturing, inertial forces play a minor role in nanorod dynamics.[8,10] Therefore, balancing the magnetic torque with the viscous torque, one obtains the governing equation describing the nanorod rotation in the film plane:[19–22]

$$\gamma\dot{\varphi} = mB\sin(\alpha - \varphi), \quad \gamma = \frac{\eta l^3 \pi}{3\ln(l/d) - A}, \quad A \approx 2.4, \qquad (1)$$

where γ is the drag coefficient, l is the nanorod length, d is its diameter. The drag coefficient was calculated based on the model of an elongated ellipsoid with a high length-to-diameter ratio. In this asymptotic case, the end effects are not important.[19] The nanorod is assumed to revolve only in the film plane without spinning around its axis. Generalization of this model to a 3-D case would require introduction of additional drag coefficients.[23] Assuming that the magnetic field is directed along the x-axis, *i.e.*, $\alpha = 0$, and φ_0 is the initial orientation of the nanorod at $t = 0$, one can solve eqn (1) analytically:[19–22]

$$t = -\frac{1}{\beta}\int_{\varphi_0}^{\varphi}\frac{\mathrm{d}\varphi}{\sin\varphi} = \frac{1}{\beta}\ln\left|\frac{1-\cos\varphi_0}{1-\cos\varphi}\frac{\sin\varphi}{\sin\varphi_0}\right|, \quad \left(\beta = \frac{mB}{\gamma}\right). \qquad (2)$$

Solution (2) suggests that the dimensionless time $T = \beta t$ for rotation of a nanorod toward its equilibrium orientation at $\varphi = 0$ depends only on the initial orientation of the nanorod, $T = T(\varphi_0)$. Eqn (2) cannot be directly used for estimation of the time needed for complete alignment of the nanorod with the field: direct substitution of $\varphi = 0$ in eqn (2) results in a singularity, *i.e.*, this time goes to infinity, $t \to \infty$.

Therefore, for practical applications of eqn (2), one can set a criterion that almost complete co-alignment of a nanorod with the field will occur if its magnetic moment is pointing toward the sector $-\Delta\varphi < \varphi < \Delta\varphi$, $|\Delta\varphi| \ll 1$. For example, taking $\Delta\varphi = 0.01$, we obtain the behavior shown in Fig. 2. The curve in Fig. 2 specifies the dimensionless time T needed for a nanorod that was initially oriented at an angle φ_0 with the x-axis, to get into the sector $-0.01 < \varphi < 0.01$. From this master curve, one can estimate the time needed for a particular nanorod to find its equilibrium orientation. For example, a nanorod at $\varphi_0 = \pm\pi/6$ to the x-axis will take about $T = 4$ dimensionless units, see the dashed lines in Fig. 2. This implies that the dimensional time to reach the equilibrium orientation $\varphi \cong 0$ will be equal to $t \cong 4/\beta$ seconds (β is measured in 1/s),

It is noteworthy that the required dimensionless time varies from zero to ten, implying that nanorods with magnetic moments antiparallel to the field would take almost ten times longer to reach the equilibrium position than nanorods whose magnetic moments start near the field direction. This observation explains the challenge of ordering an assembly of nanorods in the film: one needs to set up a criterion for nanorod alignment that will guarantee that all nanorods present will be captured and aligned along the field during nanocomposite processing.

Kinetics of alignment of nanorods assemblies

It is natural to follow the rotation of a nanorod assembly by introducing the orientational distribution function F:

$$\mathrm{d}N(\varphi) = N_t F(\varphi, t)\mathrm{d}\varphi, \qquad (3)$$

where $\mathrm{d}N(\varphi)$ is the number of nanorods whose major axes are oriented within the angle φ and $\varphi + \mathrm{d}\varphi$, N_t is the total number of nanorods in the film and $F(\varphi, t)$ is the distribution function. According to this definition, the distribution function describes the density of nanorods sitting within the angle φ and $\varphi + \mathrm{d}\varphi$. If the nanorods are initially randomly distributed, the distribution function is constant, $F(\varphi, 0) = 1/2\pi$. If at a certain moment of time $t_{\|}$, all nanorods were to point in the direction of an external field oriented at angle α with the x-axis, the distribution function would transform into the delta function $F(\varphi, t_{\|}) = \delta(\varphi - \alpha)$. Any distribution function distinct from these two limiting functions will describe a system of partially aligned nanorods.

Fig. 3 illustrates random, normal and delta distributions of nanorods in a field applied in the direction of the positive x-axis, $\alpha = 0$. The centers of mass of all nanorods were fixed at the nodes of a two-dimensional square lattice.

To describe the evolution of the distribution function with time we employ the equation of particle conservation. The most general form of this equation reads $N_t\partial F/\partial t + \nabla\cdot J = 0$. In our particular case, when the nanorods are allowed to spin only in the plane and are not engaged in translational movement, the divergence operator is reduced to $\nabla = \partial/\partial\varphi$ and the φ-component of the flux is defined as $J_\varphi = N_t F\mathrm{d}\varphi/\mathrm{d}t$. Thus, the governing equation for the distribution function is written as

$$\frac{\partial F(\varphi, t)}{\partial t} + \frac{\partial}{\partial\varphi}\left[F(\varphi, t)\dot{\varphi}\right] = 0. \qquad (4)$$

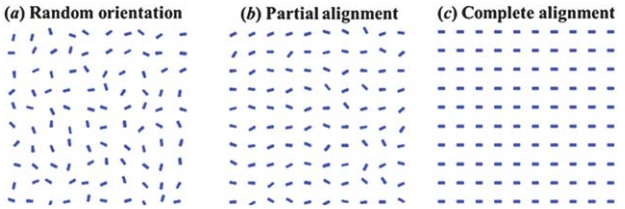

Fig. 3 Visualization of three different distribution functions describing (a) random orientation of nanorods $F(\varphi) = 1/2\pi$; (b) a normal distribution of nanorod orientations $F(\varphi) = (2/\pi^{0.5})\exp(-2\varphi^2)$, exhibiting partial alignment of nanorods in the x-direction; (c) complete alignment of nanorods in the x-direction, $F(\varphi) = \delta(\varphi)$.

Substituting eqn (1) into eqn (4), we obtain[24]

$$\frac{\partial F(\varphi,\ t)}{\partial t} + \frac{\partial}{\partial \varphi}\left[F(\varphi,\ t)\beta\ \sin(\alpha - \varphi)\right] = 0. \tag{5}$$

The differential eqn (4) describes the evolution of the distribution function under an external magnetic field directed at angle α with respect to the x-axis. The evolution of F is specified by the initial condition $F(\varphi,\ 0) = 1/2\pi$ implying a random orientation of nanorods at the first moment of time. Numerical analysis of this equation has been performed in ref. 24 for some particular examples. Here we show that eqn (5) can be solved analytically by the method of characteristics.[25]

Following the trajectory determined by eqn (2), and choosing $\alpha = 0$, the characteristic curve[25] for eqn (5) is written as

$$\mathrm{d}t = \frac{\mathrm{d}\varphi}{-\beta\ \sin\ \varphi} = \frac{\mathrm{d}F(\varphi,\ t)}{F(\varphi,\ t)\beta\ \cos\ \varphi}. \tag{6}$$

Integrating eqn (6) and taking into account the initial condition $F(\varphi,\ 0) = 1/2\pi$, we obtain

$$F(\varphi,\ t) = \frac{1}{2\pi}\frac{2C}{(C^2 - 1)\cos\ \varphi + (C^2 + 1)}, \tag{7}$$

$$C = \exp(-\beta t). \tag{8}$$

All physical parameters are collapsed into a single parameter β. Then, if one keeps the β-parameter constant, one should observe consistent kinetics. For example, if one changes the field $\boldsymbol{B}$ and fluid viscosity η keeping their ratio constant, the kinetics should not change. As follows from eqn (7) and (8), as time goes to infinity, all nanorods tend to align in the direction of the magnetic field, $F(\varphi,\ \infty) = \delta(0)$.

Fig. 4(a) illustrates the dependence of $F(\pi/8,\ t)$, $F(\pi/4,\ t)$, $F(\pi/2,\ t)$ and $F(3\pi/4,\ t)$ as functions of the dimensionless time T. Due to initial conditions, these functions start from the same value, $F(\pi/8,\ 0) = F(\pi/4,\ 0) = F(\pi/2,\ 0) = F(3\pi/4,\ 0) = 1/2\pi$. However, the evolution of these functions is very much different: we observe non-monotonous behavior of the distribution function with a maximum for the nanorods positioned within a certain angle. One can specify this angle and time to reach this maximum concentration by using solution (7) and (8). The time at which the distribution function $F(\varphi,\ t)$ reaches its maximum value is determined as $\partial F(\varphi,\ t)/\partial t = 0$, where F is given by eqn (7) and (8). Calculating this derivative, we obtain

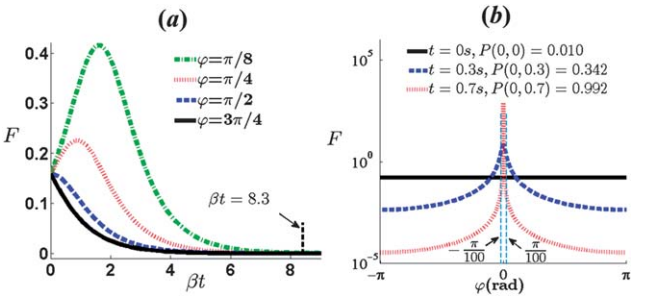

Fig. 4 (a) Dependence of $F(\pi/8,\ t)$, $F(\pi/4,\ t)$, $F(\pi/2,\ t)$ and $F(3\pi/4,\ t)$ as functions of dimensionless time $T = \beta t$; (b) profile of distribution function $F(\varphi,\ t)$ at three different time moments $t = 0$ s, $t = 0.3$ s, and $t = 0.7$ s.

$$\beta t = \frac{1}{2}\ \ln\left(\frac{1 + \cos\ \varphi}{1 - \cos\ \varphi}\right). \tag{9}$$

Because βt must be greater than zero, the argument under the logarithm must be greater than one, implying that the maximum is reached within the semi-plane $(-\pi/2,\ \pi/2)$.

As shown in Fig. 4(a), the population of nanorods within this semi-plane first increases and then decreases; the maximum is observed within the time interval between $T = 0$ and $T = 4$. Fig. 2 gives a hint for explaining this maximum. According to this master curve, the majority of nanorods require time $4 < T < 6$ to reach the equilibrium. The nanorods taking much longer time, $T > 6$, and much shorter time, $T < 4$, to reach the equilibrium are a minority. Therefore, the majority of nanorods starting outside the semi-plane $(-\pi/2,\ \pi/2)$ would pass this semi-plane within the time interval $T < 4$. Therefore, if an observer were to watch the nanorods passing by a certain sector $\varphi = \varphi_{\mathrm{observer}}$ in the semi-plane $(-\pi/2,\ \pi/2)$, he should be looking for a majority of nanorods crossing this sector at a certain time t corresponding to the maximum of $F(\varphi_{\mathrm{observer}},\ t)$.

Fig. 4(b) illustrates the angular dependence of the function $F(\varphi,\ t)$ at different moments in time; three snapshots were taken at the times $t = 0$ s, $t = 0.3$ s and $t = 0.7$ s. The parameter β was set as $\beta = 12.1\ \mathrm{s}^{-1}$. One can see that the distribution function gradually changes from a constant to a delta function. These three distribution functions exactly correspond to the respective states (a), (b) and (c) in Fig. 3.

In some applications, the full width at half maximum (FWHM) of the distribution function is of interest.[24] This function can be found analytically as follows. According to solution (7), the maximum correspond to $F(0,\ t) = 1/(2\pi C)$. Therefore, the FWHM of the distribution is obtained as the solution to equation $\cos\ \varphi = (1 - 3C^2)/(1 - C^2)$, resulting in the formula for the FWHM as

$$w = 2\mathrm{arc}\ \cos\frac{1 - 3\ \exp(-\beta t)}{1 - \exp(-\beta t)}. \tag{10}$$

This explicit formula relates the physical parameter β with the FWHM at different time moments.

Analyzing the kinetics of alignment of an assembly of nanorods, it is more convenient to deal with the probability

$P(\varphi, t)$ to find the nanorods positioned within a narrow angle, $[\varphi - \Delta\varphi, \varphi + \Delta\varphi]$. This probability $P(\varphi, t)$ is defined as

$$P(\varphi, t) = \int_{\varphi-\Delta\varphi}^{\varphi+\Delta\varphi} F(\varphi', t)\mathrm{d}\varphi' = \frac{1}{\pi}\mathrm{arc\,tan}\left[\frac{\tan(\varphi'/2)}{C}\right]\Bigg|_{\varphi-\Delta\varphi}^{\varphi+\Delta\varphi}. \quad (11)$$

Due to this definition, the probability $P(\varphi, 0) = \Delta\varphi/2\pi$ corresponds to the initial random orientation of nanorods. As time goes to infinity, the probability goes to one, $P(0, \infty) = 1$, which means that all the nanorods can be found within interval $[-\Delta\varphi, \Delta\varphi]$. One can examine a critical probability P_0 introducing it as follows: if $P(0, t) > P_0$, *i.e.* if the total number of nanorods positioned outside the interval $[-\Delta\varphi, \Delta\varphi]$ is negligibly small $(1 - P_0) \ll 1$, one can say that almost all nanorods are aligned with the field. Using this alignment criterion, we can specify the time τ needed to reach this level of alignment. One can estimate this time by substituting P_0 into the left hand side of eqn (11) and solving for time τ:

$$\tau = \frac{1}{\beta}\ln\left[\frac{\tan(\pi P_0/2)}{\tan(\Delta\varphi/2)}\right]. \quad (12)$$

Insets in Fig. 4(b) specify the probability values showing that almost complete alignment was reached within $\tau < 0.7$ seconds for the particular set of parameters $\beta = 12.1\ \mathrm{s}^{-1}$ and $\Delta\varphi = \pi/100$.

Experimental

Nanorod synthesis and surface modification

Nickel nanorods were synthesized inside pores of alumina membranes (Whatman Ltd.) using an electrodeposition technique described in detail in ref. 5, 8, 10 and 26. We exactly followed the procedure described in the supporting information of ref. 8. This experimental protocol enables one to produce nanorods with a narrow size distribution (Fig. 5).

Applying 1.5 DC voltage for 12 minutes, we obtained nanorods of about 5 μm in length and less than 200 nm in diameter. The magnetic properties of these nanorods were analyzed using an alternating gradient magnetometer (AGM MicroMag 2900 by Princeton Measurements Inc.). These nanorods are ferromagnetic; magnetic hysteresis of a 50 μg powder sample of electrodeposited nickel nanorods is shown in Fig. 6(a). In Fig. 6(b), we plot the magnetization curve in the millitesla range of the magnetic field, which is less than the coercive force. In this field range, the average magnetization is linearly dependent on the field.

To improve the dispersibility of the nanorods, we formed an adsorption layer of polyvinylpyrrolidone (PVP) on their surfaces following the protocol in ref. 27. In brief, the alumina membrane holding the synthesized nanorods was placed in 1 M solution of sodium hydroxide containing 20 mg mL^{-1} of PVP (3500 Da). After complete dissolution of the membrane, the nanorods were separated by decanting the solution and transferred into pure deionized water by several centrifugation–decanting–dispersion cycles. TEM images (STEM-Hitachi HD2000) confirm formation of the PVP polymer layer (Fig. 7). The thickness of this layer varies in the range of 40–70 nm.

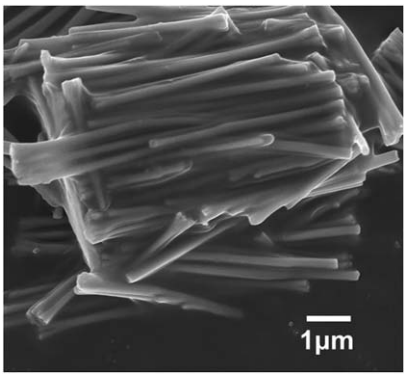

Fig. 5 SEM image of nickel nanorods.

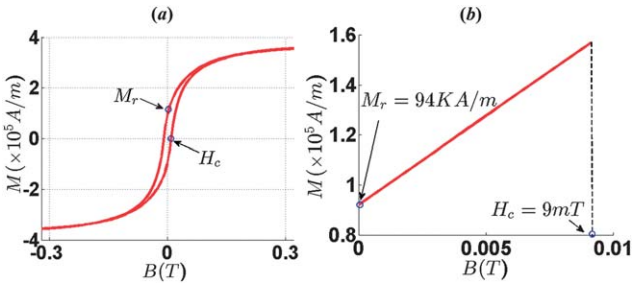

Fig. 6 (a) Full hysteresis loop obtained from the 50 μg nanorod powder sample. (b) Magnetization curve in 0–10 mT range showing linear magnetization behavior.

The functionalized nanorods were dispersed in water. The concentration of the nanorods in water was 0.04 wt%. One mL of a water-based dispersion was centrifuged for 1 min at 10 000 rpm. Then water was partially replaced with 0.1 mL of pure glycerol (Fisher Scientific Inc.). This dispersion was sonicated at 80 °C for 15 minutes. Using a refractometer (Spectronic Instruments 336410) we measured the amount of water remaining in the vial. We centrifuge the sample again and measure the refractive index of only the water–glycerol mixture. It was found to be 1.4634 at 23 °C, corresponding to a mixture of 93 wt% glycerol in water.[28] The weight concentration of nanorods of the resulting dispersion was then estimated to be 0.3 wt%. A 1 μL drop of the glycerol–water mixture containing

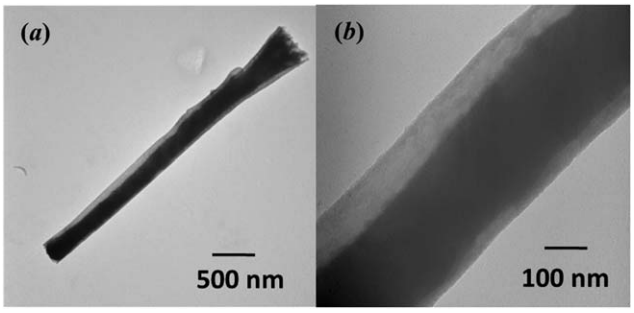

Fig. 7 TEM images of a Ni nanorod covered with a PVP layer: (a) overall view and (b) close-up.

0.3 wt% of nanorods was placed on a glass slide and immediately covered with another glass slide to prevent evaporation of water. Two glass slides were separated by two parallel 25 μm fibers, which provided a liquid film thickness of 25 μm. The visual appearance of polymer-stabilized nanorods in the glycerol–water mixture was significantly better. Observation in the dark field mode (Olympus BX 51) detected no aggregation of nanorods.

Alignment of nanorods in magnetic field

To generate a magnetic field, we used two magnetic coils placed parallel to each other and fixed under a BX-51 Olympus microscope equipped with a SPOT videocamera (SPOT Imaging Solutions, Inc.) The magnetic field was measured using a digital teslameter (133-DG GMW Inc.); and the field in the center of the optical cell was equal to 0.3 mT which is much weaker than the coercive force shown in Fig. 6(b). Therefore, the model with magnetic moment fixed at the easy axis seems to be adequate for description of the nanorod rotation. A schematic of the experimental setup is shown in Fig. 8.

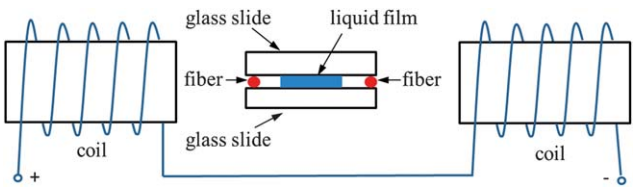

Fig. 8 Schematic of the experimental setup.

The video was recorded after switching on the coils. The field was switched off only when all the nanorods were completely aligned along the field direction.

Nanorods start to rotate as soon as the field is turned on and stop spinning when the field is switched off. The final alignment of nanorods persists for a long time; small thermal fluctuations in the nanorod position and orientation do not destroy this orientation during the observation time. A video showing the reaction of a single selected nanorod on the field can be found in the ESI (S1†). These observations support the model.

To analyze the kinetics of alignment of the nanorod assemblies, the video was transformed into a sequence of frames by the VirtualDub software (http://www.virtualdub.org). The frames taken at time moments $t = 0$ s, 1 s, 2 s, 3 s and 4 s were saved for further analysis, Fig. 9. Analyzing five frames, we selected nanorods that were present in the observation plane in all five frames. Only nanorods having the same length ($l \approx 5$ μm) were selected for the analysis. This selection allowed us to follow the theory not considering the effect of particle polydispersity. Nanorods coming into and/or leaving the observation plane during the observation period were not counted.

Prior to the analysis of the distribution function, we determined the parameter β by following the rotation of individual nanorods from the recorded video and fitted each trajectory using eqn (2) by adjusting the value of β. The experimental

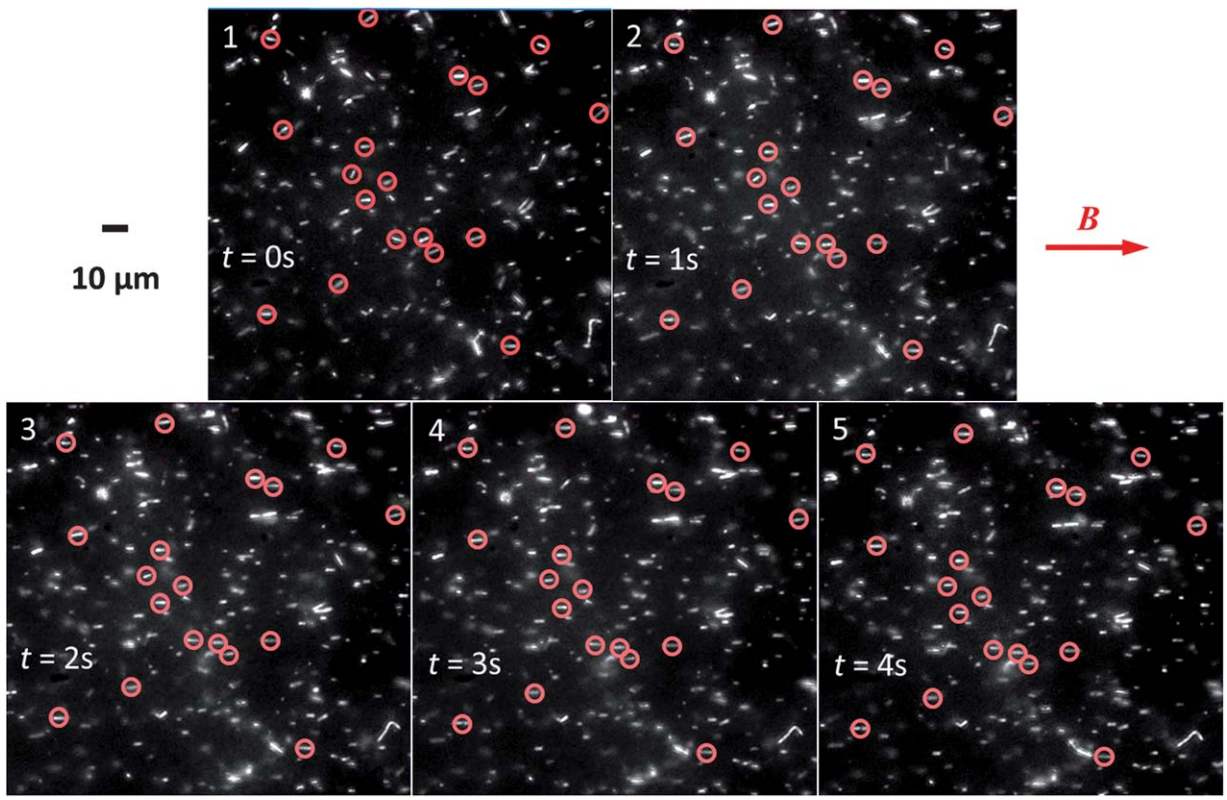

Fig. 9 Five frames chosen for analysis of the distribution function; circled nanorods were tracked during the analysis.

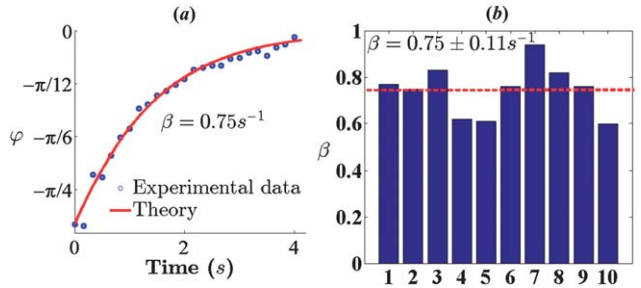

Fig. 10 (a) Nanorod trajectory (solid line) and the experimental points used for extraction of the β-parameter using eqn (2); (b) β-parameters for ten nanorods.

values of the angle φ as a function of time for individual nanorods are shown in Fig. 10. The theoretical trajectory plotted with $\beta = 0.75\ s^{-1}$ closely follows the experimental dependence.

Ten individual nanorods were tracked and the corresponding β-chart is shown in Fig. 10(b) providing an average value of $\beta = 0.75 \pm 0.11\ s^{-1}$. The standard deviation is caused by variation in the nanorod lengths and diameters; this can be inferred from the explicit expression for the β-parameter $\beta = MB[3\ln(l/d) - A][4\eta(l/d)^2]$, where M is the saturation magnetization of nickel. It is seen that the β-parameter is very sensitive to the aspect ratio l/d. As the thickness of polymer coating and nanorod length vary from one nanorod to another, this parameter changes. Nevertheless, the standard deviation is small suggesting that the average value is reliable, and the interactions between nanorods are not significant. Observe that most nanorods in Fig. 9 stay separated from each other confirming that the dispersion was stable and that interactions between the nanorods were negligible.

These observations and experimental results on alignment kinetics of individual nanorods support the hypothesis that the nanorod colloid should behave as a system of non-interacting nanorods. This hypothesis also agrees with Onsager's theory of isotropic–nematic transition in a system of rigid nanorods.[29,30] For the nanorods with diameters of 200 nm and lengths of 5 μm, the critical volume fraction for the isotropic phase is numerically estimated to be $C_{iso} = 3.3 \times 0.2/5 = 0.132$.[30] The density of a glycerol–water mixture containing 93 wt% of glycerol at 23 °C is 1.24 g mL^{-1}.[31] In a 0.3 wt% dispersion of nickel nanorods (density of nickel is 8.90 g cm^{-3}) the volume fraction of nickel nanorods is estimated to be 4×10^{-4}, which is well below the Onsager limit. Therefore, the nanorods are not touching each other.

We further examined the hypothesis of non-interacting particles by quantitatively evaluating the distribution function and comparing it with the theoretically derived one. In the analysis, we examined five movies taking five frames corresponding to the same time moments as those shown in Fig. 9. Then we tracked 14 nanorods present in each frame resulting in 70 nanorods per chart as shown in Fig. 11.

Fig. 11 summarizes the results of this analysis. The histograms represent experimental data given in terms of the

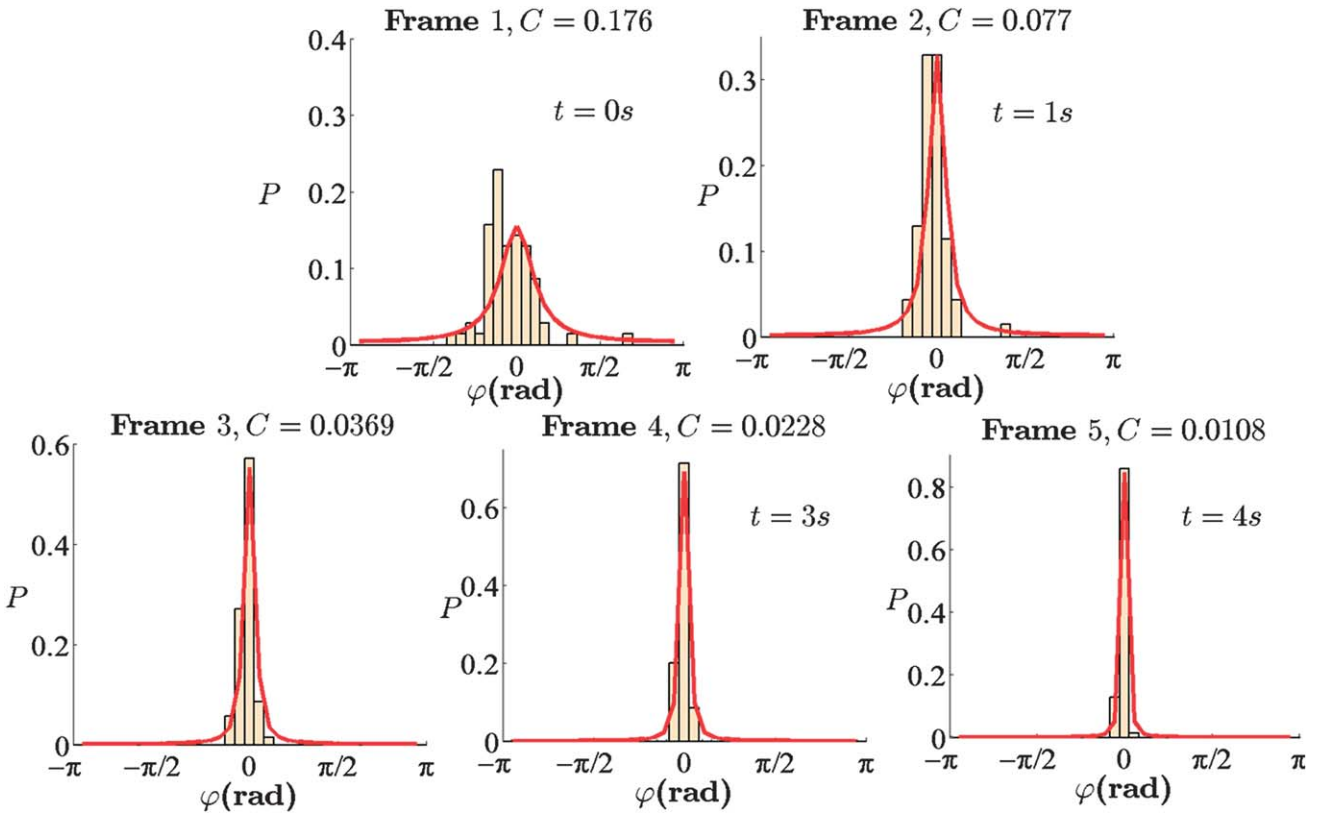

Fig. 11 Orientation distribution for nickel nanorods at $t = 0$ s, 1 s, 2 s, 3 s and 4 s. Solid curves correspond to the theoretical curves.

probability function $P(\varphi, t)$ defined by eqn (11). Experimental histograms were constructed by counting the number of nanorods N_φ present in each sector $(\varphi - \Delta\varphi, \varphi + \Delta\varphi)$ with $\Delta\varphi = \pi/36$ and normalizing N_φ by the total number of nanorods N_t present in all five pictures. Then the histograms were fitted with eqn (11) by adjusting parameter C. For each frame, we have a unique parameter C corresponding to the given shape of the probability function. As seen from Fig. 11, the solid theoretical curves agree well with the experimental results.

It is worth recalling that the theoretical model assumes that the nanorods were randomly distributed in the first moment, $F(\varphi, 0) = 1/2\pi$. However, when the cover slide was placed on the droplet, it caused some flow orienting the nanorods in the film. Therefore, the nanorods were not randomly distributed in Frame 1, which we took as the initial moment. To satisfy the initial condition of the model, we shifted time to start at an arbitrary t_0 and followed the same form of C defined by eqn (8):

$$C = \exp[-\beta(t + t_0)]. \quad (13)$$

With this definition of the C-function, the initial time moment corresponds to $t = t_0$, a new adjustable parameter. Fig. 12 shows the C-parameters corresponding to the snapshots in Fig. 11. These C-parameters appear to sit on the same curve defined by eqn (12) with parameters $\beta = 0.77\ s^{-1}$ and $t_0 = 2.3$ s. The value of the β-parameter is very close to the value obtained by tracking individual nanorods and using eqn (2) to fit the data, Fig. 10. This confirms that the nanorods do not interact with each other.

Double checking the results, one can calculate the time needed to reach the equilibrium configuration setting the criterion $P_0 = 0.9$ and $\Delta\varphi = \pi/36$ in eqn (11) and using Frame 5 in Fig. 9 as the final state. For a colloid with parameters $\beta = 0.77\ s^{-1}$ and $t_0 = 2.3$ s, this time τ was calculated from eqn (11) as $\tau = 6.5$ s. The duration of five frames is therefore estimated to be $\tau - t_0 = 6.5–2.3 = 4.2$ s, which matches the experimental value of 4 s. Thus, the proposed theory describes the experimental observations fairly well, suggesting that the nanorods do not interact with each other and that their alignment kinetics depends on the initial distribution.

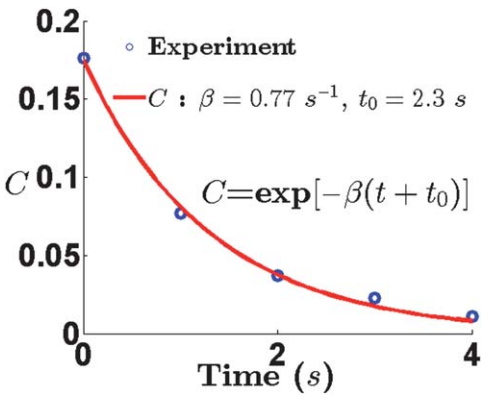

Fig. 12 A set of C-parameters extracted from Fig. 11. The solid curve shows the exponential function (13).

Conclusions

We describe the alignment kinetics of an assembly of non-interacting magnetic nanorods suspended in a Newtonian fluid with constant viscosity η and subject to an external magnetic field $\boldsymbol{B}$. It has been shown that the alignment kinetics is controlled by a single parameter β. We theoretically predicted and experimentally confirmed that one can control the alignment of an assembly of nanorods by choosing the parameter β and time of application of the external field. Experiments with nickel nanorods covered with 0.3 wt% PVP in a glycerol–water mixture supported the theory.

Acknowledgements

We thank Vladislav Vekselman for fruitful discussions and constructive suggestions. We also thank Zhaoxi Chen for taking SEM images for us. This work was supported by the Air Force Office of Scientific Research, Grant numbers FA9550-12-1-0459 and FA8650-09-D-507 5900.

Notes and references

1 S. Q. Song, G. Bohuslav, A. Capitano, J. Du, K. Taniguchi, Z. H. Cai and L. Sun, *J. Appl. Phys.*, 2012, **111**, 056103.
2 A. K. Salem, C. F. Hung, T. W. Kim, T. C. Wu, P. C. Searson and K. W. Leong, *Nanotechnology*, 2005, **16**, 484–487.
3 A. K. Wanekaya, W. Chen, N. V. Myung and A. Mulchandani, *Electroanalysis*, 2006, **18**, 533–550.
4 P. D. McGary, L. W. Tan, J. Zou, B. J. H. Stadler, P. R. Downey and A. B. Flatau, *J. Appl. Phys.*, 2006, **99**, 08B310.
5 A. Tokarev, B. Rubin, M. Bedford and K. G. Kornev, *AIP Conf. Proc.*, 2010, **1311**, 204–209.
6 A. A. Kayani, K. Khoshmanesh, S. A. Ward, A. Mitchell and K. Kalantar-Zadeh, *Biomicrofluidics*, 2012, **6**, 031501.
7 C. Wilhelm, F. Gazeau and J. C. Bacri, *Phys. Rev. E: Stat., Nonlinear, Soft Matter Phys.*, 2003, **67**, 061908.
8 A. Tokarev, I. Luzinov, J. R. Owens and K. G. Kornev, *Langmuir*, 2012, **28**, 10064–10071.
9 A. Celedon, C. M. Hale and D. Wirtz, *Biophys. J.*, 2011, **101**, 1880–1886.
10 A. Tokarev, B. Kaufman, Y. Gu, T. Andrukh, P. H. Adler and K. G. Kornev, *Appl. Phys. Lett.*, 2013, **102**, 33701.
11 L. V. Nikitin, L. S. Mironova, K. G. Kornev and G. V. Stepanov, *Polym. Sci., Ser. A*, 2004, **46**, 301–309.
12 G. Filipcsei, I. Csetneki, A. Szilagyi and M. Zrinyi, *Adv. Polym. Sci.*, 2007, **206**, 137–189.
13 R. M. Erb, R. Libanori, N. Rothfuchs and A. R. Studart, *Science*, 2012, **335**, 199–204.
14 K. Itoh, S. Ishida, M. Hamada and S. Ogawa, *J. Appl. Phys.*, 1979, **50**, 2396–2398.
15 T.-W. Chou, *Microstructural Design of Fiber Composites*, Cambridge University Press, Cambridge, UK, 1992.
16 H. J. Richter, *IEEE Trans. Magn.*, 1993, **29**, 2185–2201.
17 H. J. Richter, *J. Phys. D: Appl. Phys.*, 1999, **32**, R147–R168.
18 A. Eiling, *J. Appl. Phys.*, 1987, **62**, 2404–2418.

19 M. Doi and S. F. Edwards, *The theory of polymer dynamics*, Paperback, with corrections, Clarendon Press, Oxford, 1988.
20 J. J. Newman and R. B. Yarbroug, *J. Appl. Phys.*, 1968, **39**, 5566–5569.
21 M. M. Tirado and J. Garciadelatorre, *J. Chem. Phys.*, 1980, **73**, 1986–1993.
22 E. Blums, A. Cebers and M. M. Maiorov, *Magnetic fluids*, Walter de Gruyter, New York, 1997.
23 A. Ghosh, P. Mandal, S. Karmakar and A. Ghosh, *Phys. Chem. Chem. Phys.*, 2013, **15**, 10817–10823.
24 C. M. Perlov and S. Middleman, *J. Appl. Phys.*, 1987, **61**, 3892–3894.
25 R. Courant and D. Hilbert, *Methods of mathematical physics*, Interscience Publishers, New York, 1989.
26 A. K. Bentley, M. Farhoud, A. B. Ellis, G. C. Lisensky, A. M. L. Nickel and W. C. Crone, *J. Chem. Educ.*, 2005, **82**, 765–768.
27 M. K. Gupta, D. D. Kulkarni, R. Geryak, S. Naik and V. V. Tsukruk, *Nano Lett.*, 2013, **13**, 36–42.
28 G. P. Association, *Physical Properties of Glycerine and Its Solutions*, Glycerine Producers' Association, 1963.
29 L. Onsager, *Ann. N. Y. Acad. Sci.*, 1949, **51**, 627–659.
30 R. F. Kayser and H. J. Raveche, *Phys. Rev. A: At., Mol., Opt. Phys.*, 1978, **17**, 2067–2072.
31 N. S. Cheng, *Ind. Eng. Chem. Res.*, 2008, **47**, 3285–3288.

